SCIEPublish

Article

Design, Building and Performance of a New Photocatalytic Reactor Using TiO_2-Coated Rings Synthesized by Plasma Electrolytic Oxidation

Hernán Darío Traid [1,2], María Laura Vera [1,2], Alexander Emanuel Kurtz [1,2,†], Anabela Natalia Dwojak [1,2] and Marta Irene Litter [3,*]

[1] IMAM—Instituto de Materiales de Misiones (CONICET-UNaM), Posadas 3300, Argentina; traidhernan@gmail.com (H.D.T.); lauravera@fceqyn.unam.edu.ar (M.L.V.); alexanderkurtz34@gmail.com (A.E.K.); anabelanataliadwojak@gmail.com (A.N.D.)

[2] Facultad de Ciencias Exactas, Químicas y Naturales, Universidad Nacional de Misiones, Posadas 3300, Argentina

[3] IIIA—Instituto de Investigación e Ingeniería Ambiental (CONICET-UNSAM), Escuela de Hábitat y Sostenibilidad, Universidad Nacional de General San Martín, Campus Miguelete, Av. 25 de Mayo y Francia, San Martín 1650, Argentina

* Corresponding author. E-mail: martalitter24@gmail.com or mlitter@unsam.edu.ar (M.I.L.)

† Present address: Instituto de Nanociencia y Nanotecnología, CNEA-CONICET, Nodo Constituyentes, Av. Gral. Paz 1499, San Martín 1650, Buenos Aires, Argentina.

Received: 6 January 2025; Accepted: 13 March 2025; Available online: 3 April 2025

ABSTRACT: An annular UV photocatalytic reactor with recirculation in batch was designed and built. The design considered low construction, simple operation and maintenance costs, availability and durability of the materials used, easy cleaning, and high standards of hygiene and safety. The TiO_2 photocatalysts were synthesized by plasma electrolytic oxidation (PEO) on commercial Ti rings were compared with coatings obtained on Ti plates as a reference, and no influence of the substrate geometry on the morphology, crystallinity, or bandgap of the coatings was observed. The efficiency of the photocatalytic reactor using 10 TiO_2-coated rings was tested by Cr(VI) transformation in the presence of EDTA. The Cr(VI) transformation after 5 h irradiation attained 95%; a rather high photocatalytic activity (62%) was maintained after the third use of the rings without reactivation of the photocatalyst. These coatings synthesized by PEO have not been applied in modular photocatalytic reactors until now.

Keywords: Annular photoreactor; Titanium dioxide; Plasma electrolytic oxidation; Heterogeneous photocatalysis; Hexavalent chromium; Anodic oxidation; Advanced oxidation processes

1. Introduction

Titanium dioxide (TiO_2) coatings have been progressively applied for various purposes such as self-cleaning, antifogging and superhydrophilic surfaces, sensors, biocompatibility applications, disinfection, and solar energy conversion [1–3]. In water treatment, TiO_2 is one of the most used photocatalysts due to its commercial availability, low cost and thermal- and photostability [4–6]. Although TiO_2 is usually used as a powder in water suspension, in recent times, thin coatings have been increasingly applied to avoid the costly separation step of the photocatalyst.

TiO_2 coatings can be obtained using various techniques. From them, titanium anodic oxidation is one of the most economical and simplest methods [7–12]. In the anodic oxidation process, a direct current is circulated through an electrolytic cell where Ti is placed as the anode. Above a certain cell voltage, a phenomenon known as plasma electrolytic oxidation (PEO) takes place, whereby electrical arcs are established in the anode surface, causing high local temperatures and current densities; as a result, porous and crystalline coatings with large surface area and a strongly bonded substrate-oxide interface can be obtained [9,10]. A suitable mechanical performance of the bond substrate-oxide avoids the loss of photocatalyst, a crucial feature for the sustainable use of reactors based on immobilized coatings [13,14].

https://doi.org/10.70322/prp.2025.10011

TiO_2 anodic coatings are usually synthesized by PEO starting from Ti plates [8,9,15]; in this case, the influence of the synthesis parameters, *i.e.*, cell voltage, current density, nature and concentration of the electrolyte, temperature, *etc.*, on the morphology, proportion of the crystalline phases (anatase/rutile) and photocatalytic activity of the coating is relatively well known [6,15–19]. However, the design of modular photoreactors often requires TiO_2 synthesized starting from substrates with different geometries to ensure the effective irradiation of the photocatalyst and a high mass transfer [20]. This applies to annular reactors, where the light source is located in the center of a tube and the supported photocatalyst is on the inner surface of the surrounding annular geometry, proving to be highly efficient [21–23]. In this configuration, TiO_2 rings can be built and suitably placed in the photocatalytic reactor. However, in the anodic oxidation process, the change in the substrate geometry (e.g., from typical plates to rings) could modify the coating characteristics, such as morphology, crystallinity and, consequently, the photocatalytic activity could be affected. In addition, the synthesis of TiO_2 coatings via the PEO technique on non-plate geometries and their application in bench-scale photocatalytic reactors has not yet been studied [24,25].

The photocatalytic reactor performance has to be tested with a suitable pollutant system. Several works of our group have shown that the Cr(VI) reduction in the presence of ethylenediaminetetraacetic acid (EDTA) as a sacrificial synergetic agent is a very good and rapid system to compare the efficiency of different photocatalysts and the loss of activity after their reuse (e.g., [15,26,27]). Cr(VI) is a very well-known toxic, carcinogenic, and mutagenic pollutant, usually found in effluents of several industries, e.g., electroplating, tanneries (coming from the oxidation of Cr(III) by operational conditions), metal finishing, electronics, pigments and paints [28]. Reduction of Cr(VI) to Cr(III) significantly decreases the toxicity, and TiO_2-heterogeneous photocatalysis has been studied for this purpose. The influence of pH, dissolved oxygen, and use of EDTA as a sacrificial synergetic agent, among other variables, on the photocatalytic performance of TiO_2 at the lab scale is well known, together with the mechanism of the photocatalytic reaction [29,30]. In the absence of electron donors, precipitation of insoluble Cr(III) species on the photocatalyst can cause its progressive deactivation. It has been proved that when EDTA is used as the sacrificial electron donor, it protects the photocatalyst by decreasing its progressive deactivation and simultaneously enhances the reaction by avoiding the recombination of electron-hole pairs [27].

Thus, this study simultaneously addresses several relatively still unexplored aspects. A PEO process was used to obtain TiO_2 coatings on commercial titanium rings. TiO_2 synthesized under the same conditions on a Ti plate was used as a reference to assess the influence of the change of the substrate geometry on the morphology and crystalline structure of the coatings. A new annular photocatalytic reactor has been designed and built using the new TiO_2-coated rings as immobilized photocatalysts. Finally, the reactor performance was tested using the model system (Cr(VI) reduction in the presence of EDTA) and evaluating the loss of photocatalytic activity due to the reuse of the photocatalyst. Until now, the application of TiO_2 coatings synthesized by PEO in annular bench-scale photocatalytic reactors has not been reported.

2. Experimental

2.1. Materials and Methods

All chemicals were reagent grade and used without further purification. Sulfuric acid (H_2SO_4, Cicarelli, San Lorenzo, 95–98%), potassium dichromate ($K_2Cr_2O_7$, Biopack, Zárate, Argentina), ethylenediaminetetraacetic acid (EDTA, Riedel de Haën AG, Seelze, Germany), diphenylcarbazide (DPC, Biopack, Zárate, Argentina), acetone (C_3H_6O, Anedra, Los Troncos del Talar, Argentina, 99.5%) and phosphoric acid (H_3PO_4, Anedra, Los Troncos del Talar, Argentina, 85%) were used. Deionized water (conductivity ≤ 0.05 μS cm^{-1}) was used. pH adjustment was made with perchloric acid ($HClO_4$, Sintorgan, Villa Martelli, Argentina, 69–72%). pH was determined with an Adwa pH-meter (model AD8000, Szeged, Hungary). For ultrasonication, a Testlab (model TB02TA, 40 KHz, Bernal, Argentina) equipment was used. Magnetic stirring was performed with an Arcano stirrer (model 78HW-1, Ciudad Autónoma de Buenos Aires, Argentina).

2.2. Synthesis of the Photocatalysts

2.2.1. Preparation of the Substrates

Commercially pure titanium Grade C-2 (TiG2, ASTM B367 [31]) was used as the substrate. Plates were obtained from a sheet (2 mm thickness), cut into 3 × 2 cm^2 pieces, and rings were obtained from a welded tube (31.75 mm external diameter and 30 mm internal diameter) cut to obtain pieces of 10 mm height. One side of the plate and the inner surface of the rings were mechanically roughed with SiC abrasive papers (Köln, Ciudad Autónoma de Buenos

Aires, Argentina) from #120 to #500. After that, the substrates were cleaned with detergent and water, sprayed with alcohol, and finally dried with hot air.

2.2.2. Preparation of the Photocatalysts by Anodic Oxidation

For anodization, a JMB direct current source (model LPS360DD, Ciudad Autónoma de Buenos Aires, Argentina) was used. The anodization conditions were defined based on previously synthesized anodic TiO_2-coated plates, which demonstrate high activity, better than that of P25 coatings under the test conditions [15,16,32]. Briefly, the photocatalysts were synthesized by PEO, using the Ti substrate as the anode, applying direct current, first at constant current density (galvanostatic, 1200 A m^{-2}) up to a cell voltage of 120 V and then at constant voltage (potentiostatic, 120 V). 1 M H_2SO_4 was used as the electrolyte, and the temperature was kept at 25 °C. The evolution of voltage and current was recorded during the oxidation every 1 s. Pt sheets were used as cathodes, placed at both sides of the plate and in the center of the Ti rings. The total anodization time was 5 min for each sample.

After anodization, the samples were rinsed with water, sprayed with alcohol, and dried using hot air. Then, the samples were submitted to a post-anodization thermal treatment at 450 °C in the air for 1 h in an electrical oven (Indef Model M05C3, Córdoba, Argentina). The heating rate was 10 °C min^{-1} and the cooling down was done inside the oven.

Based on the reactor design (see Section 2.3 later), 10 TiG2 rings were anodized. Each ring was labeled with the letter "R" followed by a correlative number 1 to 10. The anodized Ti plate, used as a reference, was labeled with the letter "P."

2.2.3. Characterization of the Photocatalysts

Another ring, synthetized under the same conditions as the others, was used for characterization measurements. The surface of the photocatalysts (TiO_2-coated plate and ring) was observed by scanning electron microscopy (SEM) using Carl Zeiss equipment (model Supra 40, Oberkochen, Germany). The images of the surface were analyzed using the ImageJ software (1.54g version). An average pore diameter was calculated, assuming circular pores, and the percentage of area covered by the pores, named as porous fraction, was calculated [16].

The crystalline structure of the oxides was identified by the glancing incidence X-ray diffraction (GI-XRD) technique, with a glancing angle of 1° (Panalytical, Empyrean, Pixel3D detector, Worcestershire, UK), using CuKα radiation at a step of 0.02º(2θ)/0.5 s. The accelerating voltage and the applied current were 40 kV and 30 mA, respectively. The anatase fraction was calculated using Equation (1):

$$X_A = 1/[1 + 2.18\ (I_R/I_A)] \pm 2\% \quad (1)$$

where X_A is the molar fraction of anatase, and I_A and I_R are the total areas of the peaks of the X-ray intensities of the anatase and rutile strongest peaks in the XRD spectrum ((101) and (110), respectively) [33].

The UV-Vis diffuse reflectance spectra (DRS) of the coatings were obtained using a UV-Vis-NIR spectrophotometer Shimadzu (UV-3600 Plus, Kyoto, Japan) equipped with an integrating sphere. $BaSO_4$ was used as the reference. The spectra were recorded at room temperature in the air. The DRS were used to obtain the bandgap value (E_g) of the samples through Tauc plots, extrapolating to zero a linear fit from a plot of $(khv)1/2$ *vs.* hv, where k is the absorption coefficient and v is the frequency [34].

2.3. Photocatalytic Reactor Setup

For the design and construction of the reactor, a concentric annular geometry with the light source placed in the center of the device was selected due to its demonstrated high energetic performance [23]. A General Electric lamp (model F8T5 BLB, Boston, MA, USA), 350–390 nm irradiation range, maximum intensity at 365 nm (see the spectrum in Figure 1), was used as the UV light source.

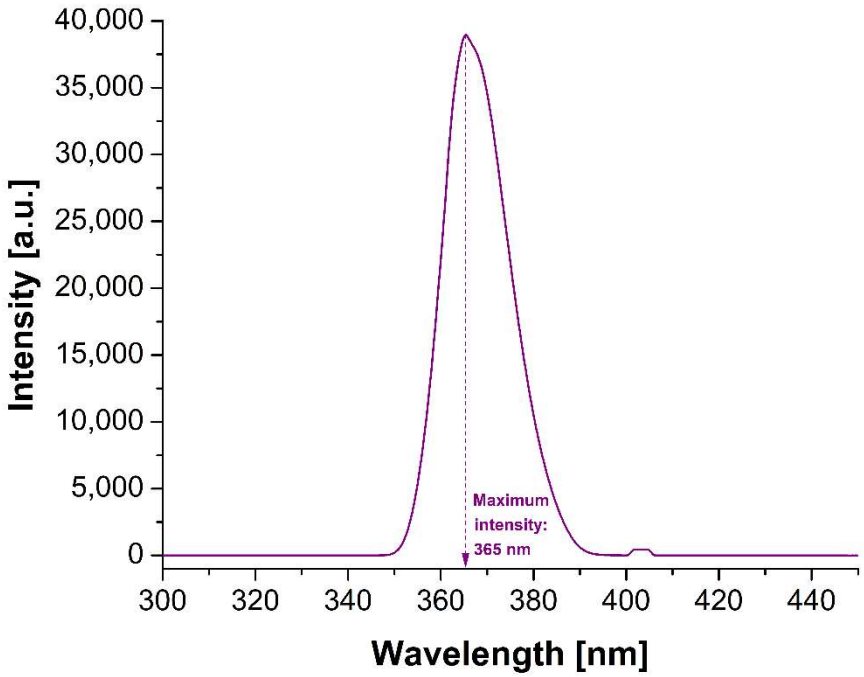

Figure 1. Spectrum of the lamp used in the annular photocatalytic reactor (GE, F8T5, BLB). Maximum intensity: 365 nm.

The reactor was built using two tubes: an inner tube made of high transparency glass (22 mm external diameter) and an outer tube made of commercial glass (37 mm external diameter), both of 2 mm thickness. The high transparency of the inner tube was verified by the determination of the irradiance at 365 nm, which presented the same value with and without the glass tube. The side and top views of the photocatalytic reactor, with the main dimensions (in mm), are presented in Figure 2.

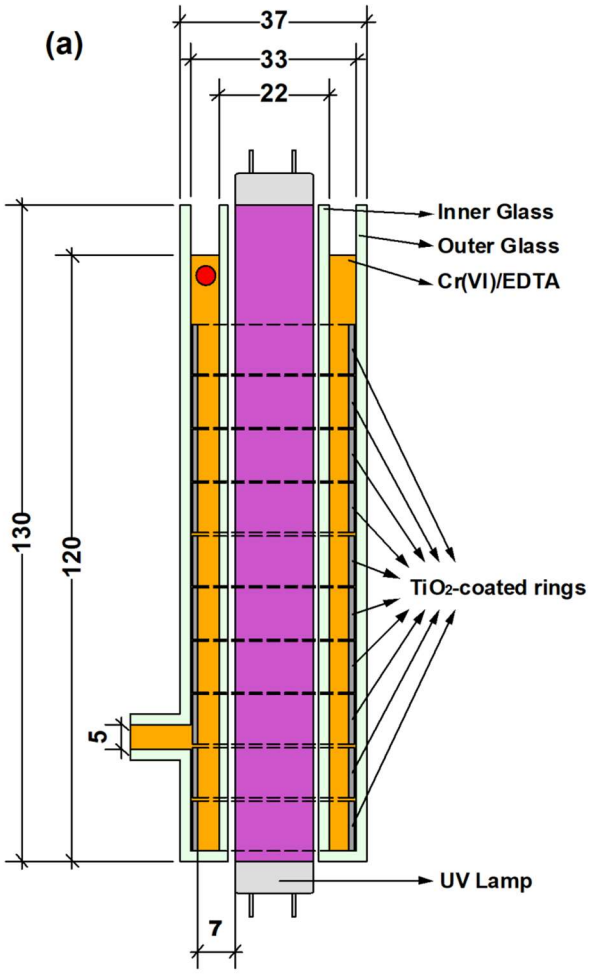

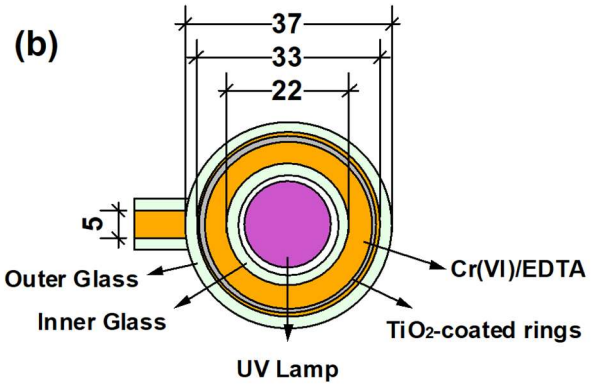

Figure 2. Photocatalytic reactor scheme: (**a**) Side view. Red circle: sampling location; (**b**) Top view. Dimensions in mm.

An irradiance of 2800 μW cm^{-2} was determined with a Spectroline radiometer (model DM-365 XA, Farmingdale, NY, USA), at 7 mm from the UV light source, which was the distance between the light source and the irradiated surface of the TiO_2-coated rings (see Figure 2a). The photocatalyst, placed between the two glasses, consisted of 10 TiO_2-coated rings (according to its capacity), providing an irradiated geometric area of ~10,000 mm^2.

To control the residence time, a closed batch flow system was adopted (Figure 3). The solution of the model pollutant was introduced axially through the open-top part of the reactor, flowing downward into the annular space between the inner glass and the inner side of the TiO_2-coated rings, and recirculated through a radial outlet (inner diameter 5 mm) in the lower part of the reactor using the peristaltic pump Watson Marlow (model 313S, Gloucestershire, UK), at a 200 mL min^{-1}.

The total volume of the suspension of the model pollutant used in the experiments was 95 cm^3 and the effectively irradiated volume (in the interior of the reactor) was 47 cm^3; it means that approximately 50% of the volume was effectively irradiated while the remaining half was outside in the recirculation system. The changes in volume of the irradiated solution with and without the TiO_2-coated rings were considered negligible. The system was refrigerated by partially submerging the recirculation circuit in a glass vessel, with water at room temperature, to keep the temperature of the system at 35 °C during the run.

Figure 3 indicates the complete irradiation setup.

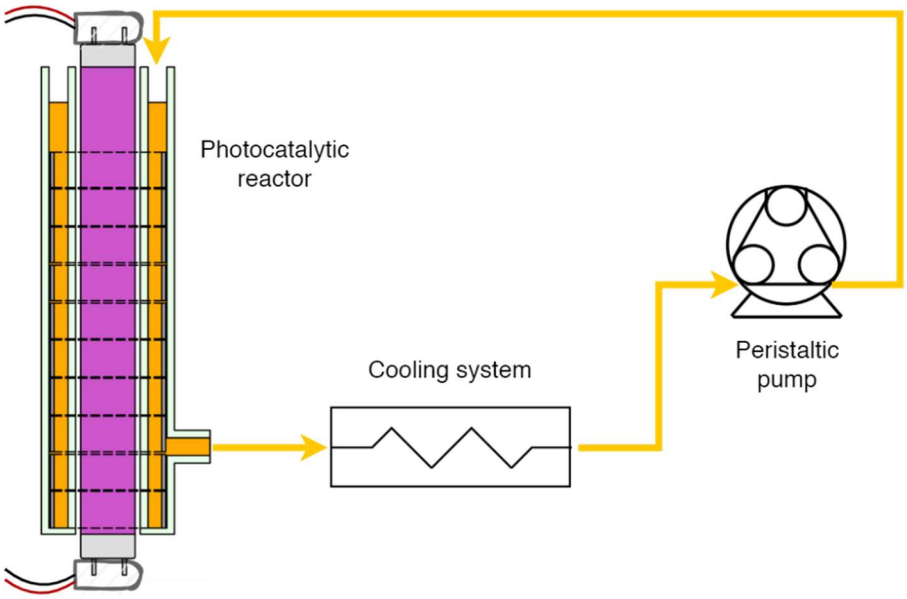

Figure 3. Photocatalytic irradiation setup.

2.4. Photocatalytic Tests

To evaluate the photocatalytic activity of the TiO_2-coated rings, tests were conducted with 10 rings placed inside the reactor (see Section 2.3). A 0.4 mM $K_2Cr_2O_7$ aqueous solution containing 1 mM EDTA at pH 2 was used as the model pollutant. Prior to irradiation, the solution was kept in the reactor with the TiO_2-coated rings in the dark for 30

minutes, to assure the adsorption equilibrium of the pollutant onto the photocatalyst surface. No significant changes in the concentration of Cr(VI) were observed after this dark period. Once the irradiation was initiated, 50 µL samples were taken periodically from the sampling point of the reactor (see Figure 2) and diluted in 3 mL of water for analysis. The irradiation was kept for 5 h. Changes in Cr(VI) concentration were monitored spectrophotometrically through the DPC method at 540 nm [35], using a Shimadzu equipment (model UV-2550, Kyoto, Japan). The homogeneous photoreduction of Cr(VI) in the system (*i.e.*, reaction in the absence of the photocatalyst) was taken as the blank. To evaluate the loss of photocatalytic activity in the TiO_2-coated rings after reuse, tests were conducted three times using the same rings. After each experiment, the reactor was disassembled, and all the pieces, including the TiO_2-coated rings, were rinsed with water and dried with hot air without further cleaning treatment. All assays were carried out in a conditioned area, bounded by fabric curtains, and opaque to UV irradiation to avoid harming people and nearby materials [32].

3. Results and Discussion

3.1. Synthesis and Characterization of the Photocatalysts

The temporal evolution of voltage and current density during the anodic oxidation process to obtain the TiO_2 photocatalysts is shown in Figures 4a and 4b, respectively. Dashed and solid lines were used for the plate (P, reference) and rings (R), respectively.

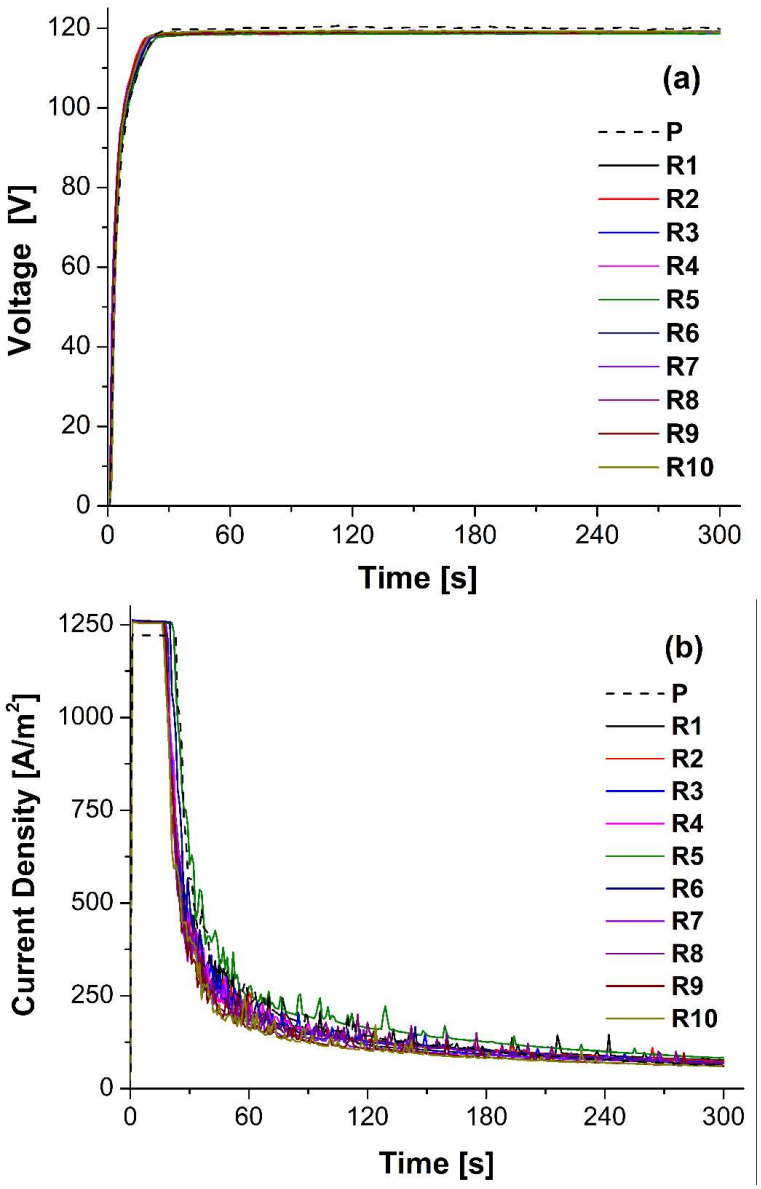

Figure 4. Anodic oxidation process to obtain the TiO_2-coated photocatalysts. Temporal evolution of: (**a**) Voltage and (**b**) Current density. Plate (P, dashed) and rings (R, solid).

The characteristic behavior of a galvanostatic-potentiostatic anodization process [10], in which a competition is established between the reactions of oxide dissolution and anodic growth of the coating [36], was observed in all curves of Figure 4. The fluctuations in current density observed in Figure 4b are the result of a substrate-oxidation-oxide breaking cycle produced by a PEO characteristic condition [37]. The overlapping of evolution curves of the "R" samples shows that the PEO of Ti substrates is a highly reproducible technique. Moreover, no difference between the curves of plates and rings was observed, indicating no influence of the substrate geometry.

The morphology of the anodic TiO_2 coatings is shown in the SEM micrographs obtained for the plate and the additional ring prepared for this measurement (Figure 5).

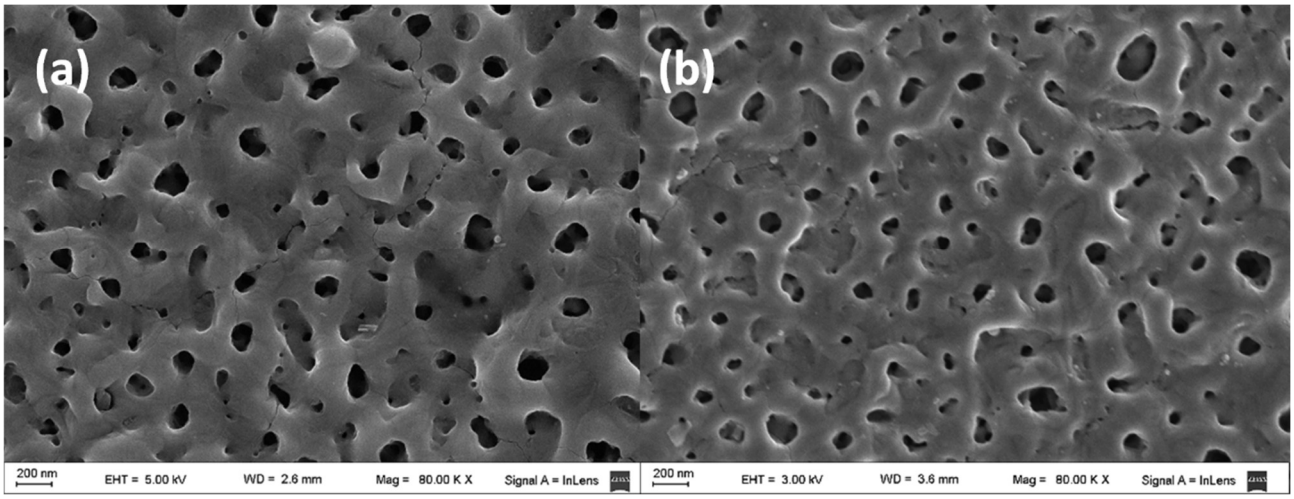

Figure 5. SEM micrographs of synthesized coatings on (**a**) Plate and (**b**) Ring.

The TiO_2 coatings show pores (dark gray) homogenously distributed on the surface, typical of PEO processes [7]. The average diameter of the pores was ~100 nm, the porous fraction was ~5% of the total surface, and the thickness (reported for coatings synthesized under the same conditions) was ~500 nm [15], as briefly described in Section 2.2.3. No differences in these parameters were found due to the substrate geometry.

Diffractograms of the samples (plate and ring), using the GI-XRD technique, are shown in Figure 6. It has been reported that TiO_2 coatings with an anatase fraction around 0.6–0.8 are more active than coatings containing the pure anatase phase [15]. In the present case, the anatase fraction was ~0.75 for both plate and ring samples, demonstrating once again no influence of the substrate geometry.

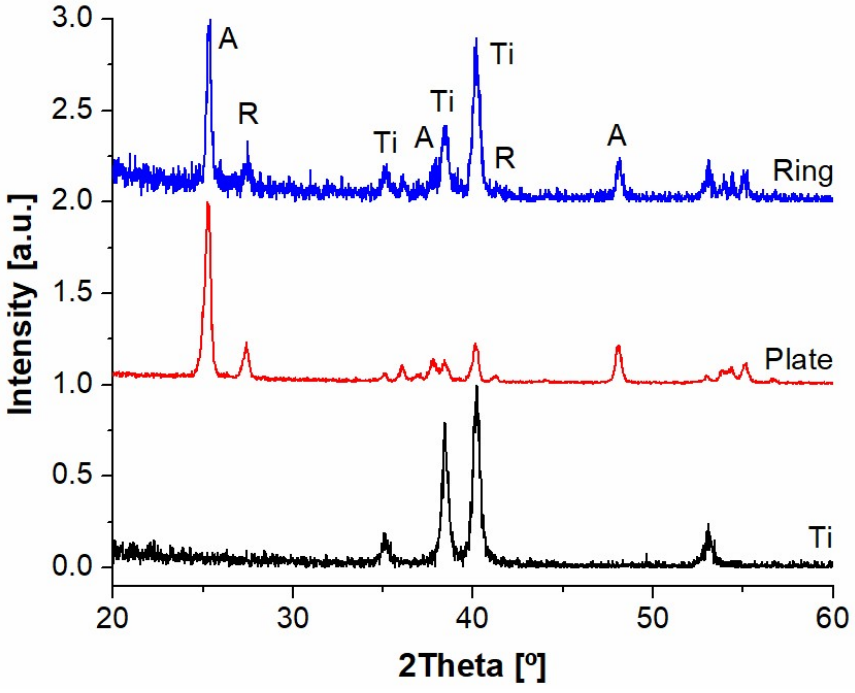

Figure 6. Normalized diffractograms of the Ti substrate and the synthesized coatings. A: anatase; R: rutile; Ti: titanium (substrate).

Bandgaps obtained by Tauc plots were also very similar for the plate and the ring, with values between 3.1 and 3.15 eV, respectively, indicated by dashed lines in Figure 7 [38].

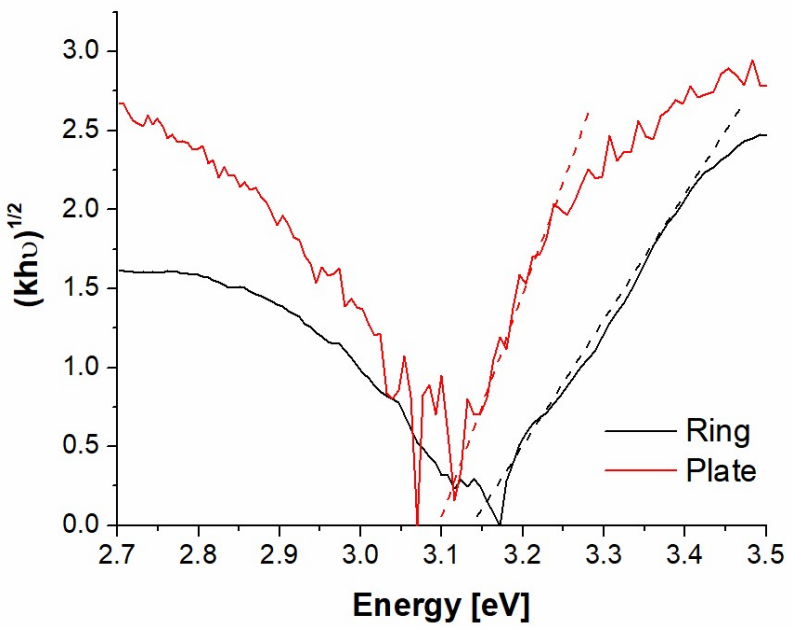

Figure 7. Tauc plots of coatings synthesized on a plate (red) and the ring (black).

3.2. Performance of the Photocatalytic Reactor

An annular reactor with immobilized TiO_2 was successfully designed and built. The entire reactor has been conceived to be affordable, from a commercially available low-cost substrate, immobilizing TiO_2 by an economical synthesis technique with high reproducibility. Additionally, low-cost materials were used for the construction of the reactor: glass, a commercial lamp, and other minor supplies. In Figure 8, a photograph of the photocatalytic irradiation setup is shown.

Figure 8. Photograph of the photocatalytic irradiation setup.

It is important to remark that the design, which takes into account operational aspects, provides four additional advantages: (1) the photocatalyst is not a structural part of the reactor, and thus, the TiO_2 coated-ring can be totally or partially replaced in a fast and easy way; (2) the modular concept of the setup allows an easy adaptation to different application needs, by changing, e.g., flow rates, available space, nature and concentration of pollutants, reaction time, *etc*.; (3) with an arrangement in parallel, it would be possible to achieve a continuous treatment system; (4) the access to the interior of reactor for an effective cleaning is very simple.

The performance of the photocatalytic reactor was tested using the 10 rings, as indicated in Section 2.4. The temporal profiles of the normalized Cr(VI) concentration for the first, second, and third use of the rings together with that of the blank (absence of photocatalyst) are presented in Figure 9. The profiles could be successfully adjusted to a first-order kinetic model, described by Equation (2) [26,39]:

$$C/C_0 = e^{-k_1 t} \quad (2)$$

where C is the Cr(VI) concentration in the solution sample at time t, C_0 is the Cr(VI) concentration at the beginning of the test, and k_1 is the first-order kinetic constant.

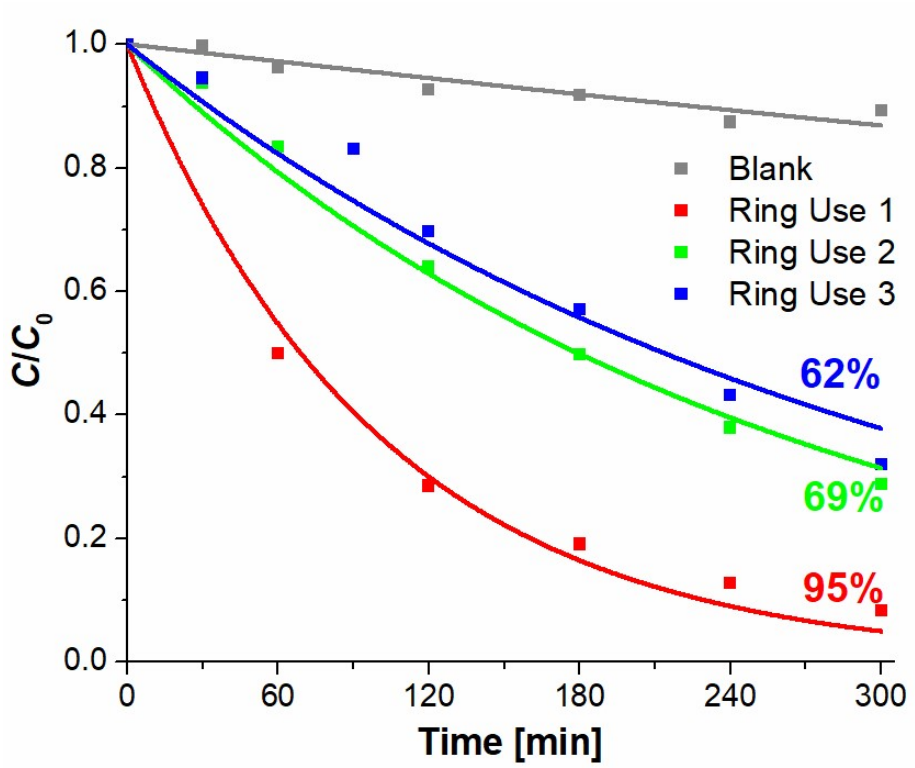

Figure 9. Temporal profiles of the normalized Cr(VI) concentration in the photocatalytic experiments of Cr(VI) transformation in the presence of EDTA under UV irradiation using 10 rings in the reactor. Results of two reuses of the same rings are also shown. Conditions: $[Cr(VI)]_0 = 0.8$ mM, [EDTA]/[Cr(VI)] = 1.25, pH 2, $E = 2800$ μW cm^{-2}, $T = 35$ °C.

The k_1 and R^2 values for the blank and each photocatalytic test with the TiO_2-coated rings are displayed in Table 1.

Table 1. First-order kinetic constant (k_1) was calculated using Equation (2), R^2 value, and percentage of Cr(VI) removal after 5 h of irradiation time. Conditions of Figure 9.

Sample	$k_1 \times 10^3$ (min^{-1})	R^2	%Cr(VI) Removal
Blank	0.47	0.90	13
First use	10.02	0.99	95
Second use	3.86	0.99	69
Third use	3.24	0.97	62

Figure 9 shows that the TiO_2 rings were rather active compared with a nearly negligible transformation in the absence of the photocatalyst. The first use of the TiO_2-coated rings shows an almost total transformation of Cr(VI) in 5 h of reaction (95%), but a progressive loss of activity (lower constant rate and %Cr(VI) removal) was observed after the subsequent two uses (Figure 9 and Table 1). It is important to point out that, although the coatings were not reactivated, they yielded a rather high transformation even during the third use (62%). Further tests are underway with

photocatalysts reactivated by washing the used coatings with water or hydrogen peroxide or by applying temperature after use, with the purpose of extending the lifetime of the photocatalyst [40–42].

During the operation, some opportunities for improvement were identified, and this will be the focus of future research. As said in Section 2.3, because half of the pollutant volume is in the irradiated tube and the other half is outside in the recirculation system, the effective irradiation time can be referred to as ~50% of the total test time (5 h). This means that if the reactor were configured to work without recirculation flow or with a lower one, the reaction time to yield the 95% removal might be significantly reduced. Another advantage of this last configuration is that the refrigeration could can be carried out simply with forced air circulation. All these features indicate that the system could be improved even more.

Finally, the operation and maintenance conditions of the system were remarkable: the reactor can be easily connected, disconnected, and cleaned. This modular design, combined with a parallel configuration of multiple photocatalytic reactors, would allow the continuous operation of a treatment system: while some reactors would be under operation, others could be cleaned and/or reactivated. The photocatalytic reactor can also be easily scaled up.

4. Conclusions

Porous TiO_2 coatings were successfully synthesized on commercially pure Ti plates and rings, applying the PEO technique with high reproducibility. The coatings synthesized on a ring or on a plate under the same anodization conditions showed no differences in morphology, crystallinity, or bandgap due to the change of the substrate geometry.

The TiO_2-coated rings were used to build a modular annular photocatalytic reactor in a closed batch flow configuration, an application not reported until now. The efficiency of the new photocatalytic reactor was tested in the reduction of an already tested model system, Cr(VI), in the presence of EDTA, using $[Cr(VI)]_0$ = 0.8 mM, [EDTA]/[Cr(VI)] = 1.25 at pH 2 under UVA irradiation (E = 2800 μW cm^{-2}). An almost complete transformation of Cr(VI) after 5 h irradiation was achieved. The photocatalytic reactor was also tested for reuse using the same TiO_2 rings; it was found that, after the third use, a rather high photocatalytic activity (62%) was still maintained, despite no reactivation of the photocatalyst.

Finally, it is important to note that this design took into consideration a low construction cost, the availability and durability of the materials used, low operation and maintenance costs, simplicity of operation and maintenance, easy cleaning and high standards of hygiene and safety. This device can be easily scaled up by enlarging the tubes and using a higher quantity of TiO_2-coated rings or by using several reactors in parallel.

Acknowledgments

The authors thank Daniel Vega from the XRD Laboratory, Department of Condensed Matter Physics, Comisión Nacional de Energía Atómica, and Enrique San Román's laboratory at Instituto de Química, Física de Materiales, Medio Ambiente y Energía, Universidad de Buenos Aires (INQUIMAE-UBA) for the DRS. All institutions are in Argentina.

Author Contributions

Conceptualization, H.D.T. and M.L.V.; Methodology, H.D.T. and M.L.V.; Validation, H.D.T., M.L.V., A.E.K., A.N.D., M.I.L.; Formal Analysis, H.D.T.; Investigation, H.D.T., M.L.V., A.E.K. and A.N.D.; Resources, M.L.V. and M.I.L.; Writing—Original Draft Preparation, H.D.T. and M.L.V.; Writing—Review & Editing, H.D.T., M.L.V. and M.I.L.; Visualization, H.D.T.; Supervision, M.L.V. and M.I.L.; Project Administration, M.I.L.; Funding Acquisition, M.L.V.

Ethics Statement

Not applicable.

Informed Consent Statement

Not applicable.

Data Availability Statement

Data is available on request.

Funding

This research was funded by Agencia Nacional de Promoción de Investigación, Desarrollo Tecnológico e Innovación (Agencia I+D+i), grants numbers PICT-2017-2133 and PICT-2017-2494.

Declaration of Competing Interest

The authors declare that they have no known competing financial interests or personal relationships that could have appeared to influence the work reported in this paper.

References

1. Zhang L, Dillert R, Bahnemann D, Vormoor M. Photo-induced hydrophilicity and self-cleaning: Models and reality. *Energy Environ. Sci.* **2012**, *5*, 7491–7507. doi:10.1039/c2ee03390a.
2. Yu H, Song L, Hao Y, Lu N, Quan X, Chen S, et al. Fabrication of pilot-scale photocatalytic disinfection device by installing TiO_2 coated helical support into UV annular reactor for strengthening sterilization. *Chem. Eng. J.* **2016**, *283*, 1506–1513. doi:10.1016/j.cej.2015.08.042.
3. Vera ML, Traid HD, Dwojak AN, Rosenberger MR, Schvezov CE. Advances in nanostructured TiO_2 coatings for industrial applications. In *Industrial Applications of Nanoparticles—A Prospective Overview*, 1st ed.; Litter MI, Ahmad A, Eds.; CRC Press: Boca Raton, FL, USA; Taylor & Francis Group: Oxfordshire, UK, 2023; Volume 1, pp. 228–255.
4. Fujishima A, Zhang X. Titanium dioxide photocatalysis: Present situation and future approaches. *C. R. Chim.* **2006**, *9*, 750–760. doi:10.1016/j.crci.2005.02.055.
5. Guo Q, Zhou C, Ma Z, Yang X. Fundamentals of TiO_2 Photocatalysis: Concepts, Mechanisms, and Challenges. *Adv. Mater.* **2019**, *31*, 1901997. doi:10.1002/adma.201901997.
6. Armaković SJ, Savanović MM, Armaković S. Titanium Dioxide as the Most Used Photocatalyst for Water Purification: An Overview. *Catalysts* **2022**, *13*, 26. doi:10.3390/catal13010026.
7. Diamanti MV, Ormellese M, Pedeferri M. Application-wise nanostructuring of anodic films on titanium: A review. *J. Exp. Nanosci.* **2015**, *10*, 1285–1308. doi:10.1080/17458080.2014.999261.
8. Sulka GD. Introduction to anodization of metals. In *Nanostructured Anodic Metal Oxides: Synthesis and Applications*, 1st ed.; Sulka GD, Ed.; Elsevier: Amsterdam, The Netherlands, 2020; Volume 1, pp. 1–34.
9. Casanova L, Arosio M, Hashemi MT, Pedeferri M, Botton GA, Ormellese M. A nanoscale investigation on the influence of anodization parameters during plasma electrolytic oxidation of titanium by high-resolution electron energy loss spectroscopy. *Appl. Surf. Sci.* **2021**, *570*, 151133. doi:10.1016/j.apsusc.2021.151133.
10. Aliofkhazraei M, Macdonald DD, Matykina E, Parfenov EV, Egorkin VS, Curran JA, et al. Review of plasma electrolytic oxidation of titanium substrates: Mechanism, properties, applications and limitations. *Appl. Surf. Sci. Adv.* **2021**, *5*, 100121. doi:10.1016/j.apsadv.2021.100121.
11. Li G, Ma F, Liu P, Qi S, Li W, Zhang K, et al. Review of micro-arc oxidation of titanium alloys: Mechanism, properties and applications. *J. Alloys Compd.* **2023**, *948*, 169773. doi:10.1016/j.jallcom.2023.169773S.
12. Makurat-Kasprolewicz B, Ossowska A. Recent advances in electrochemically surface treated titanium and its alloys for biomedical applications: A review of anodic and plasma electrolytic oxidation methods. *Mater. Today Commun.* **2023**, *34*, 105425. doi:10.1016/j.mtcomm.2023.105425.
13. Dwojak AN, Vera ML, Traid HD, Rosenberger MR, Schvezov CE, Litter MI. Photocatalytic and mechanical properties of immobilized nanotubular TiO_2 photocatalysts obtained by anodic oxidation: A novel combined analysis. *Photochem. Photobiol. Sci.* **2022**, *21*, 1793–1806. doi:10.1007/s43630-022-00257-5.
14. Manassero A, Satuf ML, Alfano OM. Photocatalytic reactors with suspended and immobilized TiO_2: Comparative efficiency evaluation. *Chem. Eng. J.* **2017**, *326*, 29–36. doi:10.1016/j.cej.2017.05.087.
15. Traid HD, Vera ML, Ares AE, Litter MI. Advances on the synthesis of porous TiO_2 coatings by anodic spark oxidation. Photocatalytic reduction of Cr(VI). *Mater. Chem. Phys.* **2017**, *191*, 106–113. doi:10.1016/j.matchemphys.2017.01.034.
16. Bayati MR, Golestani-Fard F, Moshfegh AZ. The effect of growth parameters on photo-catalytic performance of the MAO-synthesized TiO_2 nano-porous layers. *Mater. Chem. Phys.* **2010**, *120*, 582–589. doi:10.1016/j.matchemphys.2009.12.005.
17. Quintero D, Galvis O, Calderón JA, Castaño JG, Echeverría F. Effect of electrochemical parameters on the formation of anodic films on commercially pure titanium by plasma electrolytic oxidation. *Surf. Coat. Technol.* **2014**, *258*, 1223–1231. doi:10.1016/j.surfcoat.2014.06.058.
18. Pesode P, Barve S. Surface modification of titanium and titanium alloy by plasma electrolytic oxidation process for biomedical applications: A review. *Mater. Today Proc.* **2021**, *46*, 594–602. doi:10.1016/j.matpr.2020.11.294.
19. Traid HD, Vera ML, Litter MI. Total Specific Energy as a New Figure of Merit for the Design of Porous TiO_2 Surfaces Synthesized via Plasma Electrolytic Oxidation. *Ind. Eng. Chem. Res.* **2023**, *62*, 7757–7762. doi:10.1021/acs.iecr.3c00386.

20. Ochiai T, Fujishima A. Design and optimization of photocatalytic water purification reactors. In *Photocatalysis and Water Purification*, 1st ed.; Pichat P, Ed.; Wiley: Hoboken, NJ, USA, 2013; Volume 1, pp. 361–376.
21. Ballari MdlM, Satuf ML, Alfano OM. Photocatalytic Reactor Modeling: Application to Advanced Oxidation Processes for Chemical Pollution Abatement. In *Heterogeneous Photocatalysis. Topics in Current Chemistry Collections*, 1st ed.; Muñoz-Batista M, Navarrete Muñoz A, Luque R, Eds.; Springer: Berlin/Heidelberg, Germany, 2020; Volume 1, pp. 265–301.
22. Escobedo S, De Lasa H. Photocatalysis for Air Treatment Processes: Current Technologies and Future Applications for the Removal of Organic Pollutants and Viruses. *Catalysts* **2020**, *10*, 966. doi:10.3390/catal10090966.
23. Sundar KP, Kanmani S. Progression of Photocatalytic reactors and it's comparison: A Review. *Chem. Eng. Res. Des.* **2020**, *154*, 135–150. doi:10.1016/j.cherd.2019.11.035.
24. Binjhade R, Mondal R, Mondal S. Continuous photocatalytic reactor: Critical review on the design and performance. *J. Environ. Chem. Eng*. **2022**, *10*, 107746. doi:10.1016/j.jece.2022.107746.
25. Abd Rahman N, Choong CE, Pichiah S, Nah IW, Kim JR, Oh SE, et al. Recent advances in the TiO_2 based photoreactors for removing contaminants of emerging concern in water. *Sep. Purif. Technol.* **2023**, *304*, 122294. doi:10.1016/j.seppur.2022.122294.
26. Vera ML, Traid HD, Henrikson ER, Ares AE, Litter MI. Heterogeneous photocatalytic Cr(VI) reduction with short and long nanotubular TiO_2 coatings prepared by anodic oxidation. *Mater. Res. Bull.* **2018**, *97*, 150–157. doi:10.1016/j.materresbull.2017.08.013.
27. Meichtry JM, Colbeau-Justin C, Custo G, Litter MI. Preservation of the photocatalytic activity of TiO_2 by EDTA in the reductive transformation of Cr(VI). Studies by Time Resolved Microwave Conductivity. *Catal. Today* **2014**, *224*, 236–243. doi:10.1016/j.cattod.2013.10.021.
28. Tumolo M, Ancona V, De Paola D, Losacco D, Campanale C, Massarelli C, et al. Chromium Pollution in European Water, Sources, Health Risk, and Remediation Strategies: An Overview. *Int. J. Environ. Res. Public Health* **2020**, *17*, 5438. doi:10.3390/ijerph17155438.
29. Litter MI. Last advances on TiO_2-photocatalytic removal of chromium, uranium and arsenic. *Curr. Opin. Green Sustain. Chem.* **2017**, *6*, 150–158. doi:10.1016/j.cogsc.2017.04.002.
30. Kleiman A, Meichtry JM, Xaubet M, Grondona D, Litter MI, Márquez A. Efficiency of cathodic arc-grown N-doped TiO_2 films for the photocatalytic reduction of Cr(VI) under UV-Vis irradiation. *J. Phys. D Appl. Phys.* **2023**, *56*, 495303. doi:10.1088/1361-6463/acf7d2.
31. *ASTM B367-22*; Standard Specification for Titanium and Titanium Alloy Castings. ASTM International: West Conshohocken, PA, USA, 2022. doi:10.1520/B0367-22.
32. Traid HD. Síntesis de recubrimientos porosos y nanotubulares de TiO_2 anódico aplicados a fotocatálisis heterogénea. PhD Thesis, Applied Science, Universidad Nacional de Misiones, Posadas, Argentina, 2018.
33. Criado J, Real C. Mechanism of the inhibiting effect of phosphate on the anatase → rutile transformation induced by thermal and mechanical treatment of TiO_2. *J. Chem. Soc., Faraday Trans. 1* **1983**, *79*, 2765–2771. doi:10.1039/f19837902765.
34. Murphy A. Band-gap determination from diffuse reflectance measurements of semiconductor films, and application to photoelectrochemical water-splitting. *Sol. Energy Mater. Sol. Cells* **2007**, *91*, 1326–1337. doi:10.1016/j.solmat.2007.05.005.
35. *ASTM D1687-17*; Standard Test Methods for Chromium in Water. ASTM International: West Conshohocken, PA, USA, 2017. doi:10.1520/D1687-17.
36. Zwilling V, Darque-Ceretti E, Boutry-Forveille A, David D, Perrin MY, Aucouturier M. Structure and physicochemistry of anodic oxide films on titanium and TA6V alloy. *Surf. Interface Anal.* **1999**, *27*, 629–637. doi:10.1002/(SICI)1096-9918(199907)27:7.
37. Vera ML. Obtención y caracterización de películas hemocompatibles de TiO_2. PhD Thesis, Science and Technology, Instituto Sabato, CNEA-UNSAM, Buenos Aires, Argentina, 2013.
38. Hanaor DAH, Sorrell CC. Review of the anatase to rutile phase transformation. *J. Mater. Sci.* **2010**, *46*, 855–874. doi:10.1007/s10853-010-5113-0.
39. Dwojak AN, Vera ML, Traid HD, Maydana MF, Litter MI, Schvezov CE. Influence of anodizing variables on Cr(VI) photocatalytic reduction using TiO_2 nanotubes obtained by anodic oxidation. *Environ. Nanotechnol. Monit. Manag.* **2021**, *16*, 100537. doi:10.1016/j.enmm.2021.100537.
40. Weon S, He F, Choi W. Status and challenges in photocatalytic nanotechnology for cleaning air polluted with volatile organic compounds: Visible light utilization and catalyst deactivation. *Environ. Sci. Nano* **2019**, *6*, 3185–3214. doi:10.1039/c9en00891h.
41. Karim AV, Krishnan S, Shriwastav A. An overview of heterogeneous photocatalysis for the degradation of organic compounds: A special emphasis on photocorrosion and reusability. *J. Indian Chem. Soc.* **2022**, *99*, 100480. doi:10.1016/j.jics.2022.100480.
42. Salaeh S, Kovacic M, Kosir D, Kusic H, Stangar UL, Dionysiou DD, et al. Reuse of TiO_2-based catalyst for solar driven water treatment; thermal and chemical reactivation. *J. Photochem. Photobiol. A Chem.* **2017**, *333*, 117–129. doi:10.1016/j.jphotochem.2016.10.015.